Contents

5 Tagging spectrometer **2**

5.1 Tagger detectors 2

5.1.1 Focal plane microscope detector 2

Chapter 5

Tagging spectrometer

Sections left out here...

5.1 Tagger detectors

5.1.1 Focal plane microscope detector

The microscope is designed to cover the region in photon energy within the primary coherent peak 8.4-9.0 GeV, with segmentation sufficient to allow running with polarized beam at the highest intensities compatible with tagging. The primary specifications for the microscope are listed in Table 5.1.

The detector consists of a packed two-dimensional array of square 2×2 mm^2 fast-green scintillating fibers arranged along the focal plane with the fiber axis aligned with the tagged electron trajectories. A single energy channel consists of a vertical stack of 5 fibers, and there are 100 such energy channels for a total of 500 fibers. The columns are bundled in rectangular blocks of 5×5 parallel fibers. The bundles are mounted individually on a rail system that allows each one to be aligned with the local electron trajectory at its position. In its nominal position on the focal plane, the 100 energy channels map onto the range 8.3 - 9.1 GeV, which fully contains the desired region 8.4 - 9.0 GeV of the polarized peak, with some room on either side. The way the fibers are mounted allows the microscope to be reconfigured for running at other photon energies, from about 6 GeV to above 11 GeV.

The scintillators are 2 cm long, and are glued at the back to clear acrylic fibers of the same cross section. The clear fibers guide the scintillation light to photosensors located out of the plane of the spectrometer, as illustrated in Fig. 5.1. The design employs silicon photomultiplier (SiPM) devices for photosensors. These relatively new devices have a unique combination of char-

Table 5.1: Specifications for the tagging microscope counters.

Parameter	Requirement
photon energy resolution	< 60 MeV rms
tagger timing resolution	< 200 ns rms
tagging efficiency in coherent peak	> 70%
maximum integrated counting rate	250 MHz (0.5 randoms/2 ns)
maximum single-channel occupation	10%
maximum tagger background fraction	1%
dynamic range in rate	$> 10^4$
gain match between channels	10%
detection efficiency for good tags	> 90%

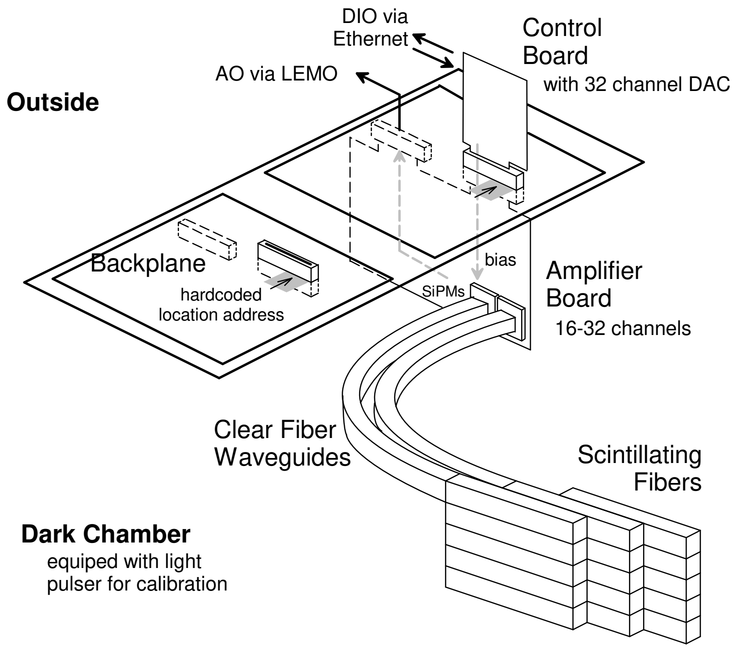

Figure 5.1: Diagram of the readout scheme of the tagger microscope. The SiPMs are connected to the scintillating fibers through clear fibers so that they can be mounted out of the radiation zone near the mid-plane of the spectrometer.

acteristics that are well suited to this application [1], [2]: gains of order 10^6, sub-ns rise time, and rate capability in excess of 10 MHz. Compared with phototomultiplier tubes, they are much more compact, which makes them ideally suited for reading out scintillating fibers. In addition, they require no high voltage and no shielding from magnetic fields, and their cost is substantially less than phototubes. The microscope requires 500 photosensors to instrument the entire array.

Extensive bench tests have been carried out on SiPM devices to confirm their suitability for use in the tagging microscope. Three different devices produced by the vendors Photonique and Hamamatsu were studied, measuring their photon detection efficiency, gain, dark rate, and inter-pixel cross talk as a function of operating temperature and bias voltage [2]. The results of this study ruled out the Hamamatsu device as unsuitable for high-rate applications[1] but the Photonique 2×2 mm^2 device what shown to meet all requirements [3].

The gain of a SiPM is quite sensitive to the applied bias voltage. The 2×2 mm^2 Photonique SiPM has a gain coefficient of 1.8/V at room temperature, which means that raising the bias voltage by 1 V increases the gain by nearly a factor 2. In addition, individual devices vary in their threshold bias voltage by as much as 2 V. Meeting the 10% gain match specification in Table 5.1 requires that the bias voltages on each SiPM be adjustable with a precision of 0.1 V. The microscope readout electronics incorporates a low-voltage supply with individual programming of the bias voltage on each SiPM in steps of 10 mV. The temperature coefficient for these SiPMs is 3%/degree, which is quite small, given the range of temperature variations that are expected in the tagger hall. Nevertheless, provision has been made to monitor local temperatures on the digital and analog readout boards.

For reasons of cost, there is only one data acquisition channel per energy channel. Each data acquisition channel consists of a flash ADC (250 MHz, 8 bit) and a constant-fraction discriminator coupled to a high-resolution TDC (50 ps least-count). Each of these sees the summed output from the 5 fibers in an energy channel. In addition, 4 columns equally-spaced along the fiber array are instrumented with separate data acquisition channels on each fiber, for a total of 120 data acquisition channels. For the column sums, each of the 5 fibers can be inhibited in the column sum simply by lowering its bias voltage below the SiPM avalanche threshold. The advantage of inhibiting some fibers

[1] Three of the Hamamatsu 400-pixel 1 mm^2 devices were tested, and all three showed anomalously frequent after-pulses with a probability distribution extending beyond 150 ns after the primary pulse.

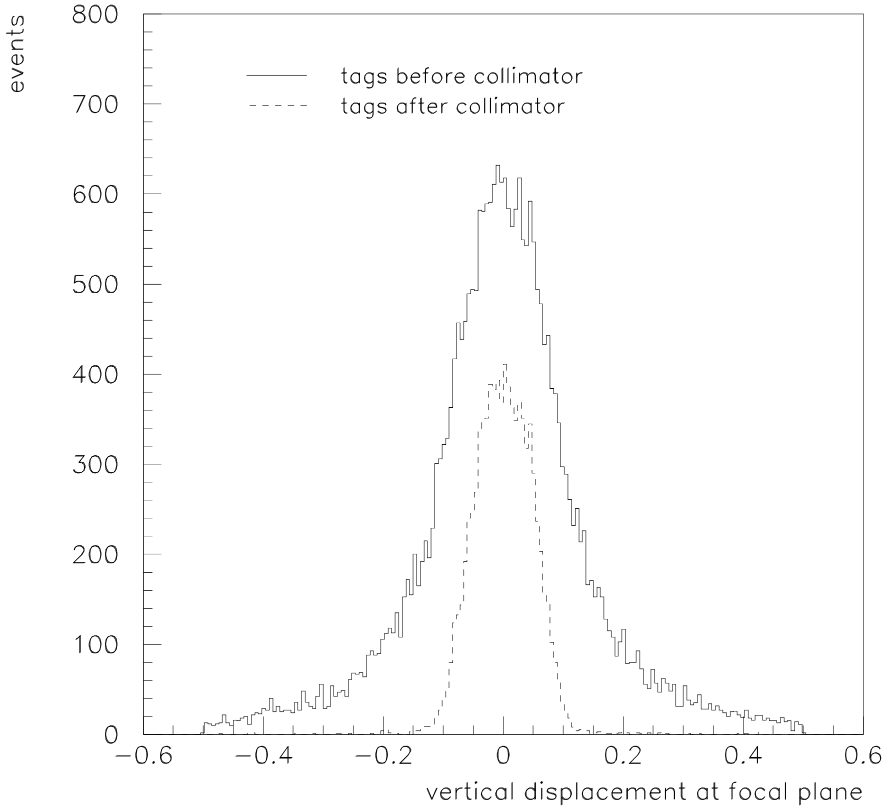

Figure 5.2: The distribution in vertical coordinate of the post-bremsstrahlung electrons at the tagger focal plane in the region of the coherent peak, for all tags (upper curve) and those that pass the photon collimator (lower curve). When all fibers except the central row in the microscope are inhibited, only electrons with $|y| < 1$ mm contribute to the tagging rate.

in each column can be seen by the two curves in Fig. 5.2. Eliminating out-of-plane electrons reduces the rate in the tagging counters by about 30%, while keeping essentially all of the tags for photons that pass the collimator.

List of Figures

5.1 Diagram of the readout scheme of the tagger microscope. The SiPMs are connected to the scintillating fibers through clear fibers so that they can be mounted out of the radiation zone near the mid-plane of the spectrometer. 3

5.2 The distribution in vertical coordinate of the post-bremsstrahlung electrons at the tagger focal plane in the region of the coherent peak, for all tags (upper curve) and those that pass the photon collimator (lower curve). When all fibers except the central row in the microscope are inhibited, only electrons with $|y| < 1$ mm contribute to the tagging rate. 5

List of Tables

5.1 Specifications for the tagging microscope counters. 3

Bibliography

[1] V. Kovaltchouk, G.J. Lolos, Z. Papandreou, and K. Wolbaum. Comparison of a silicon photomultiplier to a traditional vacuum photomultiplier. GlueX-doc-265, 2004.

[2] I. Senderovich and R.T. Jones. Suitability of silicon photomultiplier devices for readout of a scintillating fiber tagger hodoscope. GlueX-doc-760, 2007.

[3] I. Senderovich and R.T. Jones. Prototype scintillating fiber tagger microscope design and construction. GlueX-doc-1074, 2008.